Dalton Transactions

RSC Publishing

PAPER

View Article Online
View Journal | View Issue

Cite this: *Dalton Trans.*, 2013, **42**, 1033

Ligand field effect tuned magnetic behaviors of two chain compounds based on Mn^{III}_3O units: from slow magnetic relaxation to metamagnetism†

Yue-Ling Bai,*[a] Xiaoli Bao,[a] Shourong Zhu,[a] Jianhui Fang[a] and Jun Tao*[b]

Received 25th August 2012,
Accepted 16th October 2012

DOI: 10.1039/c2dt31944f

www.rsc.org/dalton

Two chain compounds built with *anti–anti* acetate bridged Mn^{III}_3O units, $[Mn_3O(Clppz)_3(EtOH)_4(OAc)]_n$ (**1**) and $[Mn_3O(Clppz)_3(EtOH)_2(OAc)]_n$ (**2**), were synthesized and characterized. The magnetic studies indicate that **1** is a single-chain magnet with two slow magnetization relaxation processes which has for the first time been found in this type of chain complex, while **2** shows a field-induced metamagnetic behavior. The quite different magnetic behaviors resulted from the different number of coordinated ethanol molecules on the Mn^{III}_3O unit, four ethanol molecules for **1**, and two ethanol molecules for **2**. The best fittings to the experimental magnetic susceptibilities gave $J_1 = -2.72$ cm^{-1}, $J_2 = -4.34$ cm^{-1}, $zJ = 1.24$ cm^{-1} for **1** and $J_1 = -5.91$ cm^{-1}, $J_2 = -0.98$ cm^{-1}, $zJ = 1.71$ for **2** above 30 K. The positive zJ values indicate the presence of weak ferromagnetic interactions between the trinuclear units *via* acetate bridges in **1** and **2**.

Introduction

The chain complexes based on the oxide-centered trinuclear manganese units $[Mn^{III}_3O]$ have been well known in recent years because their magnetic properties can be modulated by small environmental changes.[1] In order to establish magneto-structural correlations, a series of related compounds,[2] especially those containing phenol–pyrazole ligands,[3] were synthesized and reported. In all the cases, the different pyrazole derivatives and bridging ligands as well as the solvent molecules exert significant influences on the structures and magnetic properties. For example, Liu *et al.* reported the impact of different bridging ligands (azide or acetate) and solvent molecules (methanol or ethanol) on the magnetic behaviors of three chain complexes based on $[Mn^{III}_3O]$ units.[4] Reedijk *et al.* studied the effects of several different substituents at the phenol ring on the structural topology and as a consequence on the magnetic properties of trinuclear manganese(III) compounds.[3] However, we earlier also reported the different steric effects of the different phenol–pyrazole derivatives, as well as coordinated methanol or ethanol molecules resulting in the different magnetic behaviors at low temperature.[5] Herein, to further investigate the factors that influence the structures and as well the magnetic properties, two chain complexes based on the *anti–anti* acetate bridged $[Mn^{III}_3O]$ units, $[Mn_3O(Clppz)_3(EtOH)_4(OAc)]_n$ (**1**) and $[Mn_3O(Clppz)_3(EtOH)_2(OAc)]_n$ (**2**) [H_2Clppz = 3-(2-hydroxy-5-chlorophenyl)pyrazole], were synthesized and characterized. The number of coordinated ethanol molecules on the $[Mn^{III}_3O]$ unit (four ethanol molecules for **1** and two ethanol molecules for **2**) has a great influence on the structures which resulted in quite different magnetic behaviors. **1** exhibits an SCM character with two slow magnetization relaxation processes, while **2** shows a field-induced metamagnetic behavior. For phenol–pyrazole based $[Mn_3O]$ systems, most studies focused on investigating the effects of different substituent groups, different bridged anions and different solvent molecules on the structure and magnetic properties. As far as we know, this work is the first report of the different number of same coordinated solvent molecules on $[Mn^{III}_3O]$ units resulting in quite different magnetic behaviors of two chain complexes.

Experimental

Materials and methods

All starting materials were purchased commercially and used without purification. The ligand 3-(5′-chloro-2′-phenol)-1*H*-

[a]*Department of Chemistry, College of Science, Shanghai University, Shanghai 200444, P.R. China. E-mail: yuelingbai@shu.edu.cn*
[b]*Department of Chemistry, State Key Laboratory for Physical Chemistry of Solid Surfaces, Xiamen University, Xiamen 361005, People's Republic of China. E-mail: taojun@xmu.edu.cn*

†Electronic supplementary information (ESI) available: 1D chains with the intra-chain hydrogen bonds, 2D packing modes and 3D supramolecular structures, ac magnetic susceptibilities, field-dependent magnetizations, IR spectra and XRD patterns of **1** and **2**. CCDC 670811 and 885762. For ESI and crystallographic data in CIF or other electronic format see DOI: 10.1039/c2dt31944f

pyrazole was prepared using a modified literature method for 3-(2′-pyridine)-1*H*-pyrazole.[6] The elemental analyses (CHN) were performed with a Perkin-Elmer 240Q elemental analyzer. IR spectra were recorded in the range of 400–4000 cm^{-1} on a Nicolet 5DX spectrometer. Powder X-ray diffraction patterns were recorded on a Rigaku D/max-2550 X-ray diffractometer with graphite monochromatic Cu-Kα (λ = 1.54056 Å) at 40 kV per 250 mA at room temperature. Variable-temperature magnetic susceptibilities in the temperature range of 2–300 K, field dependence of magnetization, FCM, and ac susceptibilities at frequencies ranging from 1 to 1500 Hz with an ac field amplitude of 3 Oe and a zero dc applied field were performed using an MPMS-XL Quantum Design SQUID magnetometer. Diamagnetic corrections were made with Pascal's constants for all the constituent atoms.

Preparation of crystalline $[Mn_3O(Clppz)_3(EtOH)_4(OAc)]_n$ (1)

An ethanol–acetonitrile (15 mL, v/v 2 : 1) solution containing H_2Clppz (0.1 mmol), NaOEt (0.2 mmol), and $Mn(OAc)_2{\cdot}4H_2O$ (0.1 mmol) was stirred for half an hour at room temperature, then the solution was filtered and the filtrate was left for slow evaporation. The brown block crystals of **1** were collected after 4 days, and dried in air. Yield: 13.4 mg. Calcd for $C_{37}H_{42}N_6O_{10}Cl_3Mn_3$ (found): C, 44.35 (44.48); H, 4.22 (4.06); N, 8.39 (8.28). IR (KBr, cm^{-1}): 3429s, 2972w, 1596w, 1552m, 1483s, 1448m, 1399m, 1333m, 1289s, 1246m, 1146s, 1084s, 1044m, 955m, 867m, 813m, 776m, 743s, 623s, 599w, 548w, 475w.

Preparation of crystalline $[Mn_3O(Clppz)_3(EtOH)_2(OAc)]_n$ (2)

An ethanol solution (8 mL) containing H_2Clppz (0.1 mmol), NaOEt (0.2 mmol), and $Mn(OAc)_2{\cdot}4H_2O$ (0.1 mmol) was stirred for half an hour. The solution was then transferred to a 25 mL Teflon-lined stainless steel vessel. The vessel was sealed and heated to 373 K for 15 h, and then cooled at a rate of 2 K h^{-1} to room temperature. Dark-red block crystals of **2** were collected by filtration. Yield: 20.2 mg. Calcd for $C_{33}H_{30}N_6O_8Cl_3Mn_3$ (found): C, 43.56 (43.32); H, 3.32 (3.24); N, 9.24 (9.33). IR (KBr, cm^{-1}): 3438s, 1596w, 1550m, 1484s, 1448m, 1400m, 1334m, 1289s, 1247m, 1146s, 1084s, 992w, 955m, 866m, 810m, 775w, 743s, 669m, 623s, 599w, 547w, 476m.

Single crystal X-ray crystallography

X-Ray crystallographic data were collected with a Mo-Kα radiation source (λ = 0.71073 Å) by using a Bruker SMART CCD diffractometer equipped with a graphite monochromator. The structures were solved by direct methods and refined by full-matrix least-squares calculations (F^2) by using the SHELXTL-97 software.[7] All non-H atoms were refined in the anisotropic approximation against F^2 for all reflections. All H atoms were placed at their calculated positions and refined in the isotropic approximation. Crystallographic data and experimental details for structural analyses are summarized in Table 1. Selected bond lengths and bond angles are given in Table 2.

Results and discussion

Crystal structures

X-ray structural analysis reveals that **1** and **2** are chain complexes which are composed of single *anti–anti* acetate bridged $[Mn^{III}{}_3O(Clppz)_3(EtOH)_n]^+$ triangular units (Fig. 1). Each Mn···Mn edge of the triangular unit is bridged by an $\eta^1{:}\eta^1{:}\mu$-pyrazole group, and each vertex is coordinated terminally by an η^1-phenolate group, thus forming a nearly planar $\{Mn_3O(N_2O)_3\}$ moiety with the central μ_3-O^{2-} ion located 0.036 Å (for **1**) and 0.028 Å (for **2**) above the $Mn^{III}{}_3$ planes. The average intracluster Mn···Mn distances are 3.270 Å for **1** and 3.278 Å for **2**. For **1** (Fig. 1a), all of three Mn^{III} ions in the unit are distorted octahedral geometries and possess similar basal planes $[N_2O_2]$, four ethanol molecules and two acetate oxygen atoms at their axial positions. For **2** (Fig. 1b), the coordination environments of the Mn^{III} ions are similar to those observed in **1** except that Mn1 and Mn3 are distorted square pyramidal configurations, two ethanol molecules and two acetate oxygen atoms locate at the vertical positions of three Mn^{III} ions in one unit. Since the number of coordinated ethanol molecules on the unit is different for **1** and **2**, different steric effects of solvent molecules exert an obvious influence on the crystal structures. In **1**, the adjacent $[Mn^{III}{}_3]$ planes locate in a glide symmetry and are parallel to each other, the Mn···Mn distance is 6.534 Å through an acetate bridge, while the $[Mn^{III}{}_3]$ planes in **2** locate in an inverse and glide symmetry and are not parallel to each other, the dihedral angle is 14.2° and the Mn···Mn distance (6.340 Å) through an acetate bridge is a little shorter than that in **1**. It should be noticed that there are intrachain hydrogen bonds between oxygen atoms of acetate groups and coordinated ethanol molecules to help stabilize the chain structures except the covalent bonds between Mn ions and

Table 1 Crystallographic data for **1** and **2**

	1	**2**
Formula	$C_{37}H_{42}N_6O_{10}Cl_3Mn_3$	$C_{33}H_{30}N_6O_8Cl_3Mn_3$
Formula weight	1001.94	909.80
Temperature, T (K)	173(2)	223(2)
Crystal system	Monoclinic	Monoclinic
Space group	$P2_1/c$	$P2_1/c$
a (Å)	7.6085(11)	15.381(2)
b (Å)	41.541(6)	16.819(3)
c (Å)	13.1293(18)	14.024(2)
α (°)	90	90
β (°)	100.939(2)	100.337(3)
γ (°)	90	90
V (Å^3)	4074.3(10)	3569.1(10)
Z	4	4
ρ (g cm^{-3})	1.633	1.693
M (mm^{-1})	1.177	1.330
Goodness-of-fit, GOF	1.337	1.116
F(000)	2048	1840
R_1 [a] $[I > 2\sigma(I)]$	0.0967	0.0634
wR_2 (all data)	0.1836	0.1553

[a] $R_1 = ||F_o| - |F_c||/|F_o|$; $wR_2 = [w(|F_o^2| - |F_c^2|)^2/w|F_o^2|^2]^{1/2}$.

Table 2 Selected bond distances (Å) and angles (°) for **1** and **2**[a]

1					
Mn(1)–O(3)	1.832(4)	Mn(2)–O(4)	1.835(4)	Mn(3)–O(2)	1.834(5)
Mn(1)–O(1)	1.890(4)	Mn(2)–O(1)	1.879(4)	Mn(3)–O(1)	1.896(4)
Mn(1)–N(4)	1.939(5)	Mn(2)–N(6)	1.942(5)	Mn(3)–N(1)	1.938(5)
Mn(1)–N(5)	1.994(5)	Mn(2)–N(2)	1.971(5)	Mn(3)–N(3)	1.984(5)
Mn(1)–O(7)	2.214(5)	Mn(2)–O(6)	2.291(4)	Mn(3)–O(5)#1	2.265(5)
Mn(1)–O(9)	2.324(5)	Mn(2)–O(8)	2.295(5)	Mn(3)–O(10)	2.273(5)
O(7)–Mn(1)–O(9)	172.2(2)	O(6)–Mn(2)–O(8)	169.47(18)	O(5)#1–Mn(3)–O(10)	168.67(19)
2					
Mn(1)–O(2)	1.836(3)	Mn(2)–O(3)	1.834(3)	Mn(3)–O(4)	1.827(3)
Mn(1)–O(1)	1.878(3)	Mn(2)–O(1)	1.901(3)	Mn(3)–O(1)	1.899(3)
Mn(1)–N(2)	1.927(3)	Mn(2)–N(4)	1.932(4)	Mn(3)–N(6)	1.935(4)
Mn(1)–N(3)	1.975(4)	Mn(2)–N(5)	1.976(4)	Mn(3)–N(1)	1.975(4)
Mn(1)–O(5)	2.093(3)	Mn(2)–O(7)	2.290(4)	Mn(3)–O(6)#1	2.133(3)
O(7)–Mn(2)–O(8)	170.39(13)	Mn(2)–O(8)	2.305(3)		

[a] Symmetry transformations used to generate equivalent atoms for **1**: #1 $x-1, y, z$. #2 $x+1, y, z$; for **2**: #1 $x, -y+1/2, z-1/2$. #2 $x, -y+1/2, z+1/2$.

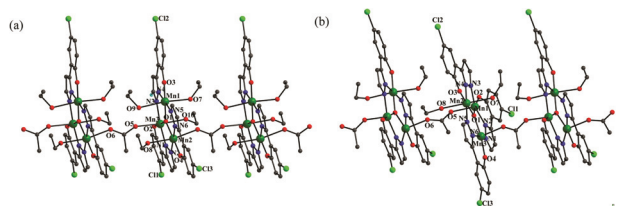

Fig. 1 1D chain structures of **1** (a) and **2** (b).

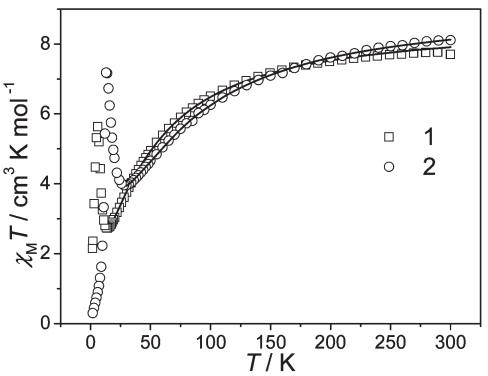

Fig. 2 Magnetic susceptibilities of **1** and **2** under applied fields of 1 kOe (**1**) and 2 kOe (**2**), respectively. The solid lines represent the theoretical fitting.

acetate groups, *i.e.*, four hydrogen bonds of O7–H···O10 [3.174(9) Å], O8–H···O5 [3.095(8) Å], O10–H···O6 [2.923(7) Å] and O9–H···O5 [2.728(7) Å] in **1** and two hydrogen bonds of O7–H···O6 [2.790(5) Å] and O8–H···O5 [2.830(5) Å] in **2** (Fig. S1†), respectively. In **2**, the dimer-like double chain structures can form through Mn···Cl weak interactions (3.316 Å) and π–π interactions (3.306 Å) between benzene rings of $Clppz^{2-}$ in neighboring chains (Fig. S3†). The shortest interchain Mn···Mn distance is 8.389 Å. While there are no predominant intermolecular weak interactions between the chains in **1**, the shortest interchain Mn···Mn distance is 10.433 Å, much larger than that in **2**, which suggests that the chains of **1** are well separated from each other. In addition, in **1**, three Mn^{III} ions in the unit show the typical Jahn–Teller elongation axes running in the chain direction, however, O_{axial}–Mn–O_{axial} bond angles and Mn–O_{axial} bond distances which are magnetically important for strong magnetic anisotropy of Mn^{III} ions are different for three Mn^{III} ions, the O_{axial}–Mn–O_{axial} angle is 172.20°, the Mn–O_{axial} distances are 2.324 and 2.214 Å for Mn1, the bond angles and distances are 169.47° and 168.67°, 2.295 and 2.291 Å, 2.265 and 2.273 Å for Mn2 and Mn3, respectively. The results for Mn2 and Mn3 look similar but a little different from those for Mn1. While in **2**, only one Mn^{III} ion shows a Jahn–Teller effect because of only two ethanol molecules on the unit. The different structural features may be the reason for the observed different magnetic behaviors for **1** and **2**.

Magnetic properties

Magnetic susceptibilities of **1** and **2** were measured under fields of 1 kG (for **1**) and 2 kG (for **2**) in the 2–300 K temperature range. The room temperature $\chi_M T$ values per Mn_3 unit are 7.70 and 8.11 cm^3 K mol^{-1} for **1** and **2** (Fig. 2), respectively, somewhat lower than the expected value of 9.0 cm^3 K mol^{-1} for three isolated Mn^{III} ions. These values decrease smoothly with deceasing temperature and reach the minimum value of 2.73 and 3.96 cm^3 K mol^{-1} at 14 and 30 K for **1** and **2**, respectively, which suggests dominant intracluster antiferromagnetic interactions. Then on lowering temperatures, the $\chi_M T$ values increase rapidly to 5.63 and 7.18 cm^3 K mol^{-1} at 6 and 13 K for **1** and **2**, respectively, and then fall abruptly, which may arise from zero-field splitting, Zeeman effects, and/or weak interchain interactions. These data of **1** and **2** were fitted to the theoretical expression for an isosceles triangle (J_1, J_2) model by treating the intrachain interunit interactions with mean field approximations (zJ),[5a] to give $J_1 = -2.72$ cm^{-1}, $J_2 = -4.34$ cm^{-1}, $zJ = 1.24$ cm^{-1}, $g = 1.96$ and $R = 7.25 \times 10^{-6}$ for **1** above 20 K and $J_1 = -5.91$ cm^{-1}, $J_2 = -0.98$ cm^{-1}, $zJ = 1.71$, $g = 2.02$ and $R = 8.19 \times 10^{-6}$ for **2** above 30 K. The positive zJ values indicate

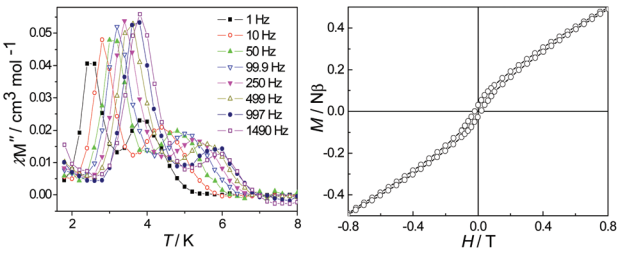

Fig. 3 Temperature dependence of χ_M'' for **1** at zero dc field and an ac field of 3 Oe (left) and the hysteresis loop at 1.8 K for **1** (right).

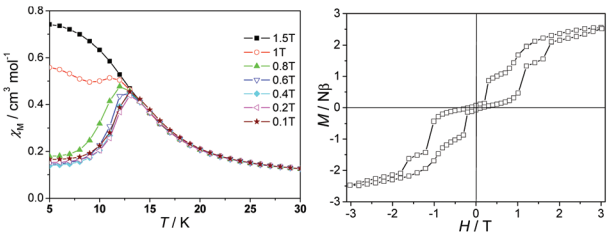

Fig. 4 Temperature dependence of the FCM at various fields for **2** (left) and the hysteresis loop at 1.8 K for **2** (right).

weak ferromagnetic interactions *via* acetate bridges, which is different from that in the ethanol analogues with Meppz and Brppz coligands in which weak antiferromagnetic interactions obviously exist.[5a,b]

The ac susceptibility data were collected in the range 1.8–8 K in a 3 G AC field oscillating at 1–1500 Hz for **1** (Fig. 3 and Fig. S4†). Both the in-phase signal (χ_M') and the out-of-phase signal (χ_M'') show strong frequency-dependence below 7 K, which is directly associated with the slow magnetization relaxation. It is unexpected that the χ_M'' exhibits an obvious magnetic susceptibility peak in the 2–4 K region and a shoulder in the 4–7 K range, which is corresponding to the low-temperature (LT) and the high-temperature (HT) phase, respectively. This phenomenon has often been observed in some Mn_{12} SMMs[8] and some other SMMs,[9] but it is relatively rare for SCMs.[10] According to the structure features, the two types of magnetic relaxation processes maybe originate from the static Jahn–Teller isomerism of Mn^{III} ions at low temperature,[8] or, it probably stems from the infinite and finite chain effects.[10a] The shift of the peak temperature (T_f) of χ_M'' can be quantified as $\varphi = (\Delta T_f/T_f)/\Delta(\log \omega) = 0.15$, which is in the range of normal superparamagnets, and excludes the possibility of a spin glass ($0.01 < \varphi < 0.1$).[11] The LT peak temperatures of χ_M'' can be fitted by the Arrhenius law $\tau = \tau_0 \exp(U_{eff}/k_BT)$, where U_{eff} is the effective relaxation barrier, τ is the relaxation time, and k_B is the Boltzmann constant, which gives U_{eff} = 49.1 K, $\tau_0 = 3.9 \times 10^{-10}$ s (Fig. S5†), respectively, thereby confirming the superparamagnetic behavior. The field-dependent magnetization at 1.8 K displays a small hysteresis with a coercive field of 190 Oe (Fig. 3, right). The dynamics of the magnetization relaxation and hysteresis of **1** suggest classical SCM character.

For **2**, the ac susceptibility measurements show that the χ_M' appears as a sharp peak at 13 K, while the χ_M'' remains zero (Fig. S6†), which indicates the transition temperature (T_N) was 13 K and excludes any glassy or superparamagnetic behaviors. The field-cooled magnetizations (FCMs) at different fields of 0.1–1.5 T also display maxima at about 13 K, and the maxima disappeared when the applied fields increased to 1.5 T (Fig. 4, left), indicating a field-induced metamagnetic behavior and the occurrence of a long-range magnetic ordering through forming a 3D supramolecular array. The plots of $M(H)$ show a sigmoidal shape (Fig. S7†), which further confirmed the metamagnetic behavior, and isothermal magnetization measurement shows a hysteresis loop with a coercive field of 140 Oe (Fig. 4, right). Furthermore, the hysteresis loop is not smooth but instead comprises plateaulike regions separated by steps which further confirms field-induced metamagnetic behavior, in addition, this phenomenon is the signature of quantum tunnelling of magnetization which often occurred in some molecular magnets.[12] Moreover, a few solids containing electronically confined magnetic nanostructures have this character.[13]

For **1** and **2**, the overall intracluster magnetic couplings are antiferromagnetic and are similar to those in most previously reported compounds with phenol–pyrazole ligands, except $[Mn_3(\mu_3\text{-}O)(phpzMe)_3(O_2CMe)(EtOH)]\cdot EtOH$[3b] and $[Mn_3(\mu_3\text{-}O)(phpzMe)_3(O_2CMe)(MeOH)_3]\cdot 1.5MeOH$,[3a] where the antiferromagnetic and ferromagnetic interactions coexist in trinuclear Mn^{III} clusters. While the intercluster ferromagnetic interactions *via* acetate bridges are found in **1** and **2**, which are as observed in methanol analogues of $[Mn_3O(ppz)_3(MeOH)_3(OAc)]_n$ and $[Mn_3O(Meppz)_3(MeOH)_4(OAc)]_n$,[5b] but are completely different from those in the alcohol analogues with Meppz, Rphpz and Brppz coligands, whose acetate bridges mediate weak antiferromagnetic interactions.[5a,3c,4b] For oxide-centered trinuclear manganese systems containing phenol–pyrazole ligands and carboxylate bridges, the SCM behaviors are often observed in compounds with ethanol as coordinated solvent molecules. In this work, the different number of coordinated ethanol molecules on the unit led to the different number of octahedral configuration manganese ions in the unit, three octahedral configuration manganese ions for **1** and one octahedral geometry manganese ion for **2**, which ultimately resulted in the different JT elongation axes running in the direction of the chains, this is the main reason for **1** and **2** to show quite different magnetic behaviors at low temperature, another reason is the different structure effects from the stacking modes and the interchain weak interactions coming from the different steric hindrance of coordinated ethanol molecules.

Conclusions

In conclusion, two chain complexes (**1** and **2**) built with $[Mn^{III}_3O]$ units were synthesized and characterized. The difference between them is the number of coordinated ethanol molecules on the unit, four ethanol molecules for **1**, and two

ethanol molecules for **2**, which produced different steric effects resulting in the different crystal structures and ultimately leading to quite different magnetic behaviors. **1** exhibits the classical SCM behavior, and it is interesting that **1** shows two slow magnetization relaxation processes which is first found in trinuclear manganese(III) compounds, while **2** shows a field-induced metamagnetic behavior. This work is the first to study the ligand field effect of the different number of same coordinated solvent molecules on unit tuned magnetic properties of the chains based on the $[Mn^{III}_3O]$ units with the same coligand and the same bridging ligand, which not only enriches the family of chains with $[Mn^{III}_3O]$ units, but also provides new examples for the study of the influencing factors on magnetic behaviors for this family.

Acknowledgements

This work was supported by the National Natural Science Foundation of China (21001073 and 20971084), the Excellent Young Teacher Foundation of Shanghai Municipal Education Commission, and the Innovation Foundation of Shanghai University. We thank Instrumental Analysis and Research Center of Shanghai University for measurements.

References

1 (*a*) J. Kim, J. M. Lim and Y. Do, *Eur. J. Inorg. Chem.*, 2003, 2563; (*b*) H.-B. Xu, B.-W. Wang, F. Pan, Z.-M. Wang and S. Gao, *Angew. Chem., Int. Ed.*, 2007, **46**, 7388; (*c*) X. Song, P. Yang, X. Mei, L. Li and D. Liao, *Eur. J. Inorg. Chem.*, 2010, 1689; (*d*) C.-I. Yang, P.-Y. Feng, Y.-T. Chen, Y.-J. Tsai, G.-H. Lee and H.-L. Tsai, *Polyhedron*, 2011, **30**, 3265.

2 (*a*) R. Inglis, L. F. Jones, G. Karotsis, S. Parsons, S. P. Perlepes, W. Wernsdorfer and E. K. Brechin, *Chem. Commun.*, 2008, 5924; (*b*) T. C. Stamatatos, D. Foguet-Albiol, C. C. Stoumpos, C. P. Raptopoulou, A. Terzis, W. Wernsdorfer, S. P. Perlepes and G. Christou, *J. Am. Chem. Soc.*, 2005, **127**, 15380; (*c*) T. C. Stamatatos, D. Foguet-Albiol, C. C. Stoumpos, C. P. Raptopoulou, A. Terzis, W. Wernsdorfer, S. P. Perlepes and G. Christou, *Polyhedron*, 2007, **26**, 2165; (*d*) C.-I. Yang, W. Wernsdorfer, K.-H. Cheng, M. Nakano, G.-H. Lee and H.-L. Tsai, *Inorg. Chem.*, 2008, **47**, 10184; (*e*) R. Inglis, S. M. Taylor, L. F. Jones, G. S. Papaefstathiou, S. P. Perlepes, S. Datta, S. Hill, W. Wernsdorfer and E. K. Brechin, *Dalton Trans.*, 2009, 9157; (*f*) R. Inglis, L. F. Jones, K. Mason, A. Collins, S. A. Moggach, S. Parsons, S. P. Perlepes, W. Wernsdorfer and E. K. Brechin, *Chem.–Eur. J.*, 2008, **14**, 9117.

3 (*a*) M. Viciano-Chumillas, S. Tanase, I. Mutikainen, U. Turpeinen, L. J. de Jongh and J. Reedijk, *Inorg. Chem.*, 2008, **47**, 5919; (*b*) M. Viciano-Chumillas, S. Tanase, I. Mutikainen, U. Turpeinen, L. J. De. Jongh and J. Reedijk, *Dalton Trans.*, 2009, 7445; (*c*) M. Viciano-Chumillas, S. Tanase, O. Roubeau, S. J. Teat, L. J. De. Jongh and J. Reedijk, *Eur. J. Inorg. Chem.*, 2010, 947.

4 (*a*) C. M. Liu, D. Q. Zhang and D. B. Zhu, *Chem. Commun.*, 2008, 368; (*b*) C. M. Liu, D. Q. Zhang and D. B. Zhu, *Inorg. Chem.*, 2009, **48**, 4980.

5 (*a*) Y.-L. Bai, J. Tao, W. Wernsdorfer, O. Sato, R. B. Huang and L. S. Zheng, *J. Am. Chem. Soc.*, 2006, **128**, 16428; (*b*) J. Tao, Y. Z. Zhang, Y.-L. Bai and O. Sato, *Inorg. Chem.*, 2006, **45**, 4877.

6 A. J. Amoroso, A. M. C. Thompson, J. C. Jeffery, P. L. Jones, J. A. McCleverty and M. D. Ward, *Chem. Commun.*, 1994, 2751.

7 G. M. Sheldrick, *SHELXTL, version 5.1*, Bruker AXS, Inc., Madison, WI, 1997.

8 (*a*) S. M. J. Aubin, Z. Sun, H. J. Eppley, E. M. Rumberger, I. A. Guzei, K. Folting, P. K. Gantzel, A. L. Rheingold, G. Christou and D. N. Hendrickson, *Inorg. Chem.*, 2001, **40**, 2127; (*b*) M. Soler, W. Wernsdorfer, K. A. Abboud, J. C. Huffman, E. R. Davidson, D. N. Hendrickson and G. Christou, *J. Am. Chem. Soc.*, 2003, **125**, 3576; (*c*) N. E. Chakov, M. Soler, W. Wernsdorfer, K. A. Abboud and G. Christou, *Inorg. Chem.*, 2005, **44**, 5304; (*d*) R. Bagai and G. Christou, *Inorg. Chem.*, 2007, **46**, 10810.

9 (*a*) Y.-N. Guo, G.-F. Xu, P. Gamez, L. Zhao, S.-Y. Lin, R. Deng, J. Tang and H.-J. Zang, *J. Am. Chem. Soc.*, 2010, **132**, 8538; (*b*) I. J. Hewitt, J. Tang, N. T. Madhu, C. E. Anson, Y. Lan, J. Luzon, M. Etienne, R. Sessoli and A. K. Powell, *Angew. Chem., Int. Ed.*, 2010, **49**, 6352; (*c*) R. Liu, L. Li, X. Wang, P. Yang, C. Wang, D. Liao and J.-P. Sutter, *Chem. Commun.*, 2010, **46**, 2566; (*d*) J. D. Rinehart, K. R. Meihaus and J. R. Long, *J. Am. Chem. Soc.*, 2010, **132**, 7572; (*e*) S.-D. Jiang, B.-W. Wang, H.-L. Sun, Z.-M. Wang and S. Gao, *J. Am. Chem. Soc.*, 2011, **133**, 4730; (*f*) Y.-N. Guo, G.-F. Xu, W. Wernsdorfer, L. Ungur, Y. Guo, J. Tang, H.-J. Zhang, L. F. Chibotaru and A. K. Powell, *J. Am. Chem. Soc.*, 2011, **133**, 11948; (*g*) P.-E. Car, M. Perfetti, M. Mannini, A. Favre, A. Caneschi and R. Sessoli, *Chem. Commun.*, 2011, **47**, 3751; (*h*) J. Ferrando-Soria, E. Pardo, R. Ruiz-García, J. Cano, F. Lloret, M. Julve, Y. Journaux, J. Pasán and C. Ruiz-Pérez, *Chem.–Eur. J.*, 2011, **17**, 2176.

10 (*a*) J. H. Yoon, J. W. Lee, D. W. Ryu, S. Y. Choi, S. W. Yoon, B. J. Suh, E. K. Koh, H. C. Kim and C. S. Hong, *Inorg. Chem.*, 2011, **50**, 11306; (*b*) J. Ferrando-Soria, D. Cangussu, M. Eslava, Y. Journaux, R. Lescouëzec, M. Julve, F. Lloret, J. Pasán, C. Ruiz-Pérez, E. Lhotel, C. Paulsen and E. Pardo, *Chem.–Eur. J.*, 2011, **17**, 12482.

11 J. A. Mydosh, *Spin Glasses: An Experimental Introduction*, Taylor & Francis, London, 1993.

12 (*a*) M. Murugesu, W. Wernsdorfer, G. Christou and E. K. Brechin, *Inorg. Chem.*, 2004, **43**, 4203; (*b*) L. K. Thompson, O. Waldmann and Z. Xu, *Coord. Chem. Rev.*, 2005, **249**, 2677; (*c*) W. L. Queen, S.-J. Hwu and L. Wang, *Angew. Chem., Int. Ed.*, 2007, **46**, 5344; (*d*) H. Miyasaka, A. Saitoh and S. Abe, *Coord. Chem. Rev.*, 2007, **251**, 2622; (*e*) J. H. Yoon, J. W. Lee, D. W. Ryu,

S. W. Yoon, B. J. Suh, H. C. Kim and C. S. Hong, *Chem.–Eur. J.*, 2011, **17**, 3028; (*f*) J. H. Yoon, W. R. Lee, D. W. Ryu, J. W. Lee, S. W. Yoon, B. J. Suh, H. C. Kim and C. S. Hong, *Inorg. Chem.*, 2011, **50**, 10777.

13 (*a*) S.-J. Hwu, *Chem. Mater.*, 1998, **10**, 2846; (*b*) S.-J. Hwu, M. Ulutagay-Kartin, J. A. Clayhold, R. Mackay, T. A. Wardojo, C. J. O'Connor and M. Krawiec, *J. Am. Chem. Soc.*, 2002, **124**, 12404; (*c*) M. Ulutagay-Kartin, S.-J. Hwu and J. A. Clayhold, *Inorg. Chem.*, 2003, **42**, 2405; (*d*) X. Mo, K. M. S. Etheredge, S.-J. Hwu and Q. Huang, *Inorg. Chem.*, 2006, **45**, 3478; (*e*) K. G. Sanjaya Ranmohotti, X. Mo, M. K. Smith and S.-J. Hwu, *Inorg. Chem.*, 2006, **45**, 3665; (*f*) S. Loth, S. Baumann, C. P. Lutz, D. M. Eigler and A. J. Heinrich, *Science*, 2012, **335**, 196.